FORMATION OF RECRYSTALLIZATION TEXTURE WITH ROLLING ORIENTATION IN Al-1.3%Mn ALLOY①

Yang Ping†, O. Engler†† and G. Gottstein†††
† *Department of Materials Science and Engineering, University of Science and Technology Beijing, Beijing 100083, P. R. China*
†† *Los Alamos National Laboratory, Center for Materials Science, Mail Stop, K765, Los Alamos, NM, 87545, USA*
††† *Institut für Metallkunde und Metallphysik der RWTH Aachen Kopernikusstr 14, D-52056 Aachen, Germany*

ABSTRACT The formation of recrystallization texture with rolling orientation (e g the *R* texture) and its influencing factors in a pure Al-1.3%Mn alloy were investigated by means of X-ray texture analysis and particularly local orientation measurements based on EBSD in SEM and MBED in TEM. The results show that this texture component is caused by the grains formed at grain boundaries through SIBM mechanism and its formation is favored by Mn atoms in solution, large initial grain size and low annealing temperature. The grains formed in this way are mainly *B*/*R* oriented and their growth is inferior to that of cube grains. The reason for the formation of such texture component is attributed to the differences in misorientations of different matrices, the deformation behavior relates to initial grain size and the Mn atoms in solution.

Key words recrystallization texture AlMn ODF

1 INTRODUCTION

In commercial pure Al (1*xxx* series) with Fe and Si, the recrystallization texture with rolling orientation, ie the *R* texture {124}⟨612⟩, often occurs at low annealing temperatures[1-4], which is very similar to the *S* component of the rolling texture. This *R* component was interpreted in two ways: either through continuous recrystallization[5] (the same orientation retained through direct subgrain growth) or due to the 40°⟨111⟩ relationship between *R* and its complementary R' component[3, 4]. Similarly, the texture component, usually *B* oriented {110}⟨112⟩, was frequently found in 3*xxx* AlMn alloys at lower annealing temperatures[5-7]. It was observed that the nucleation of grains with rolling texture orientations began earlier than that of cube grains[6] and by comparing the color contrast of grains under polarized light through anodic oxidation, it was suggested that such grains formed by SIBM (Strain induced boundary migration).

This *B*-, or *R*-component, existed at large strain, was also detected in Al-1.3% Mn alloy and this study aims to find out, firstly, its influencing factors and, secondly, to clarify on microscale the nucleation sites of the grains and their growth characteristics by means of microtexture analyses, e g EBSD (Electron back-scattering diffraction) in SEM or MBED (Microbeam electron diffraction) in TEM.

2 EXPERIMENTAL

From high purity Al with 1.3%Mn, three specimens with different precipitation states were prepared:

(1) The single phase sample A0 solutioned at 630 ℃ and then water quenched;

① Project 97-832 supported by the Science Foundation of Education Ministry of China for Outstanding Young Teachers
Received Oct. 22, 1997; accepted Feb. 1, 1998

(2) Two phases, particle-containing (Al_6Mn) sample A170 prepared from sample A0 by aging at 400 ℃ for 170 h; samples A0 and A170 were then exposed to a series of three-axial forgings and annealings to minimize the influence of initial texture and to reduce the initial grain size;

(3) Another piece of sample A170 was further annealed at 628 ℃ for 24 h to obtain a large initial grain size (called sample A200).

The initial grain sizes of three samples A0, A170 and A200 were 120, 40 and 120 μm and their initial textures were weak inverse Goss texture (4.5x), weak cube texture (2.8x), and weak cube texture (3.3x) (intensity in ODF), respectively.

These samples were cold rolled to thickness reductions of 80% ~ 97% in accordance with the condition for homogeneous rolling[8] and, then, were subjected to annealing in a salt bath. Macrotextures were determined by measuring pole Figs. on the automated X-ray texture goniometer Autex III[9]. From the measured pole Figs., ODFs were calculated according to the series expansion method[10]. Local orientations were obtained by EBSD[11] or MBED. Gauss ODFs were calculated by associating each single orientation with a Gauss type peak with a scatter width of 5°.

3 RESULTS AND ANALYSES

3.1 Influencing factors of recrystallization textures with rolling orientation

The recrystallization texture with rolling orientation was found prevailingly in the samples A0 with Mn atoms in solution. Fig. 1 shows the macrotextures of recrystallized samples A0, indicating the influences of strain and annealing temperature. It can be seen that besides the cube texture {100}〈001〉, the recrystallization texture with rolling orientation, which was mainly

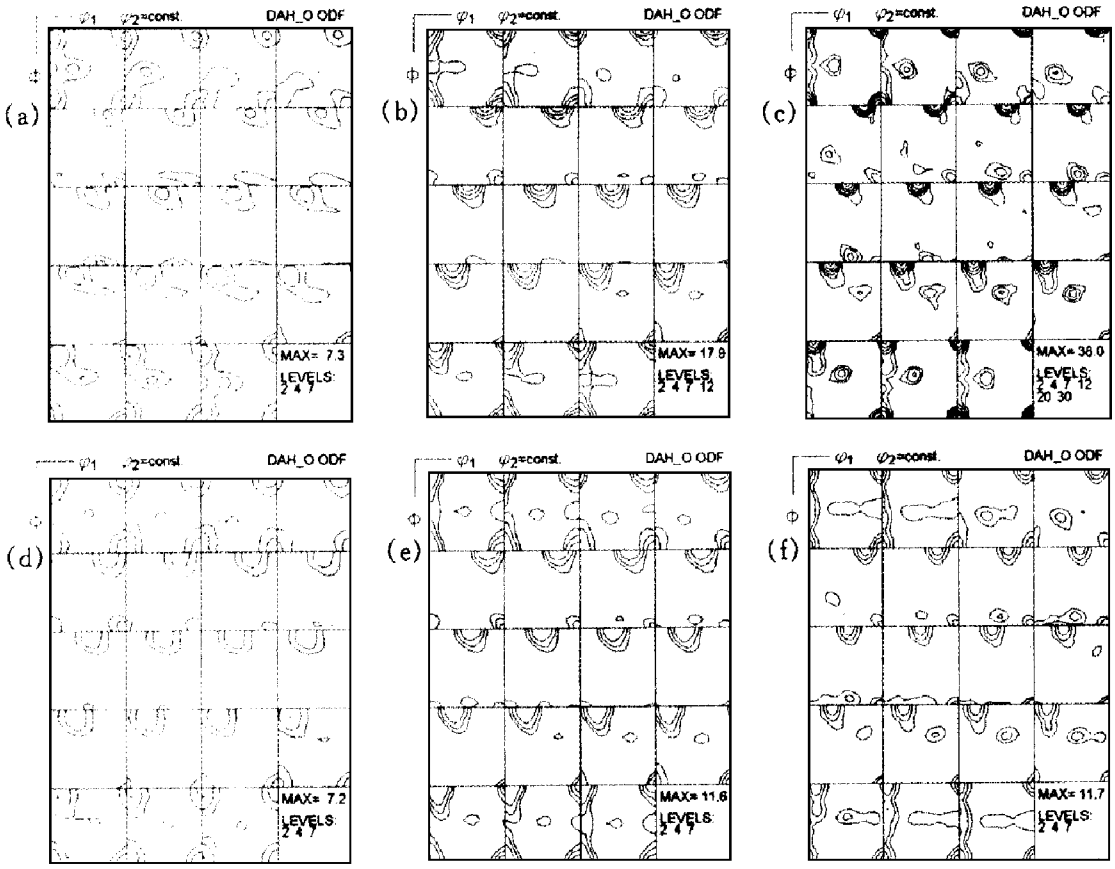

Fig. 1 Recrystallization textures in samples A0 rolled at different reduction ratios and annealing temperatures

(a) —80%, 375 ℃; (b) —92%, 375 ℃; (c) —97%, 375 ℃; (d) —80%, 450 ℃; (e) —92%, 450 ℃; (f) —97%, 450 ℃

B-oriented in 80% rolled sample and *R*-oriented in 97% rolled sample, was the second prominent texture component and its intensity increases at large strain and low annealing temperature.

Such texture component has not been detected in the particle-containing samples A170 and A200 by X-ray analysis. However, local orientation analysis revealed the differences by measuring the orientations of new grains formed at early stages of recrystallization in three different samples (80% rolled, 380 ℃, 20s annealed A0; 86% rolled, 350 ℃, 30 s annealed A170 and 82% rolled, 350 ℃, 25 s annealed A200) and grouping the grains according to their orientations. The results are shown in Fig. 2 (For the samples containing particles (A170 and A200) only the grains formed far away from particles were considered). Some significant distinctions were found:

(1) In the sample A0 with a large initial grain size (120 μm), the orientation distribution of the new grains (Fig. 2(a)) and structural observation indicated that the *B* component was produced by the nucleation at grain boundaries. Furthermore, the intensity of *B* component (12. 3*x* random) was even higher than that of the $cube_{RD}$ and $cube_{TD}$ one (~ 6*x* random). At 380 ℃, 32. 6% of the new grains were cube oriented with $Cube_{RD}$ and $Cube_{RD}$ scattering (within 20° scattering), 38. 9% were *B*-oriented grains (or 46. 5% were grains with rolling texture orientations). There were still 20. 9% randomly oriented grains, which should also mostly originate from the nucleation at grain boundaries.

(2) In the sample A170 with a small initial grain size (40 μm), the orientations of all new grains (Fig. 2(b)) demonstrated clearly that, besides the $cube_{RD}$ and $cube_{TD}$ components, which were related to the nucleation at cube bands[12] (26. 4% grains in number within 20° scattering), the grains formed at grain boundaries did not produce strong texture components (only 3. 1% new grains were *B*-oriented and 64. 4% grains were randomly oriented). That means, even in microscale the rolling texture component did not emerge.

(3) In the sample A200 with a large initial grain size (120 μm), no strong texture component occurred (Fig. 2(c)). However, a weak *B* component occurred including 15. 7% of all the grains in number (or 27. 1% of the grains of rolling texture orientations). The remaining 57. 2% were randomly oriented.

3.2 Growth of new grains with rolling orientations analyzed by local orientation measurements

In the newly formed grains with rolling orientations, SIBM process was often observed. This can be proved easily by referring either to their morphologies or to their orientation relationships with matrices. As shown in Fig. 3, the new grain 1 has the same *B* orientation as subgrains 2~ 5. Thus, it must be formed by the subgrains within the *B* oriented band grew into

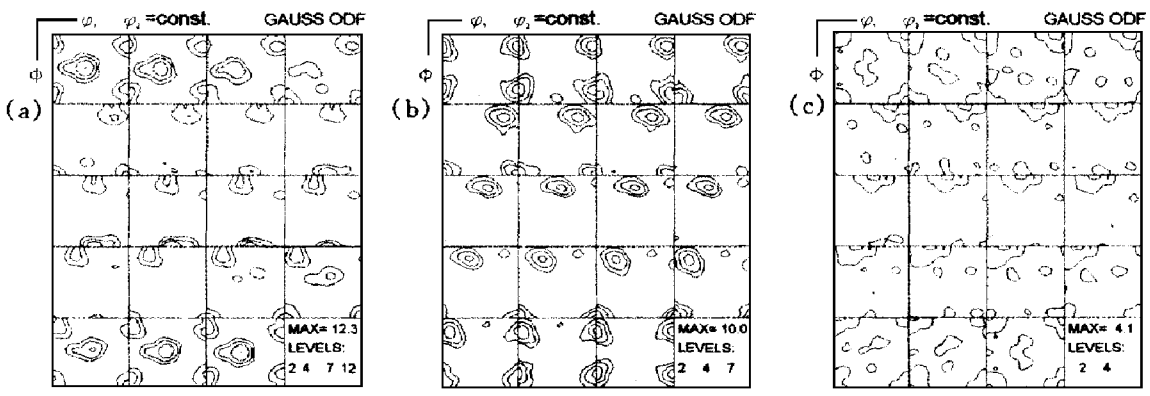

Fig. 2 Orientation distributions of grains at early stages of recrystallization in three samples
(a) —80%, 380 ℃, 20s, A0; (b) —86%, 350 ℃, 30s, A170; (c) —82%, 350 ℃, 25s, A200

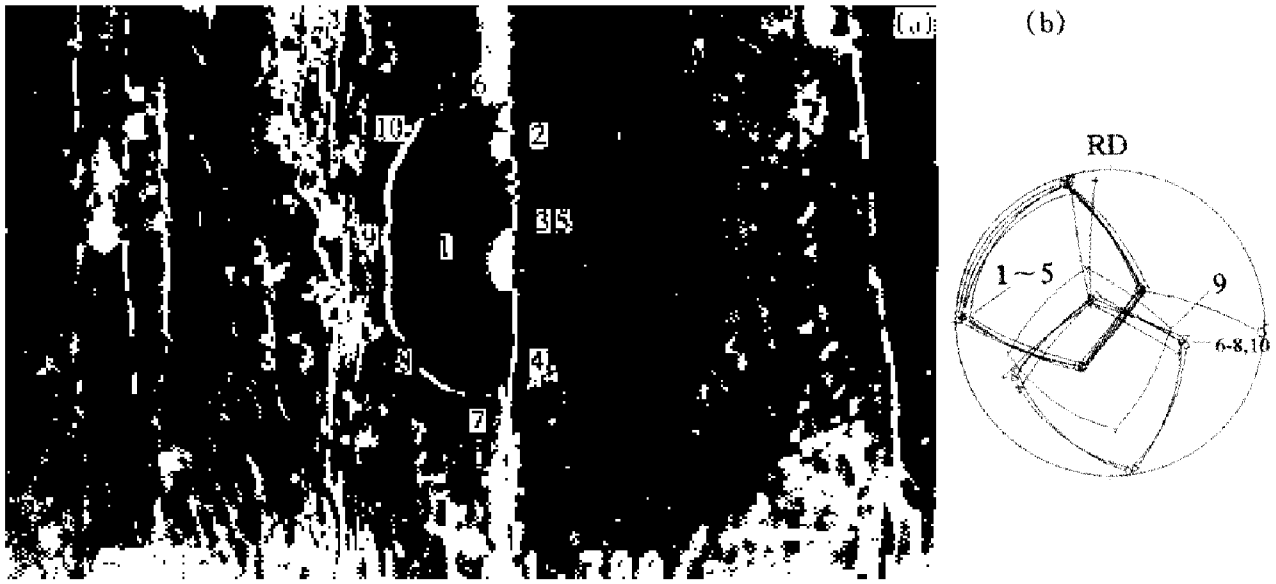

Fig. 3 An example of an SIBM-grain in 80% rolled and 400 ℃, 10 s annealed sample A0

the other, namely *S* oriented grain.

In addition to the predominant features of SIBM grains (their unidirectional growth and their resemblance in orientation to their parent grains), there are some other features. In most cases, SIBM grains formed in groups as shown in Fig. 4, illustrating a group of *B*-grains (1~3) grew into a rotated *G* matrix. This reveals a high nucleation rate and hence explains the large number of such grains at the early stage of recrystallization in samples A0 annealed at low temperatures. The growth feature of SIBM grains in groups can also be determined by measuring the orientation relationships among the recrystallized grains. The grains with Σ– 1 relationships (small angle grain boundary) are often *B*/*R* oriented (or cube oriented), indicating the nucleation feature in groups. Fig. 5 exhibits another growth feature of SIBM grains. The recrystallized grains (1~ 3, 10, 11) grew into a *C*-oriented deformation band. At this time only a small part of the deformed matrix of this band (12~ 14) can be seen. The feature of the unidirectional growth of SIBM grains vanished at this stage. However, the orientation relationships show clearly that the *B* oriented grains 2, 3 originated either from the deformation band on the left (4, 5, 9) or on the right (6~ 8) by SIBM, while the grains 10, 11 stemmed from the matrix, which was located above or below this section. Due to the complementary relationship of grains 10, 11 with both *B* deformation bands 4~ 9 (60° ⟨111⟩ stable, immobile twin boundary) they can not grow into the other two *B* bands, but only into the *C* oriented band (12~ 14). According to Taylor models[13], in order to fulfill the compatibility, the banding of *B* grains proceeds parallel to the longitudinal section into two complementary parts (so it is normally difficult to detect them morphologically in longitudinal sections). Such complementarily oriented *B* bands were observed[14] in the rolling plane. Grains 1, 2 were a twin pair.

TEM observations indicated that in Fig. 6, two SIBM grains (1, 2) with an *R* orientation formed. The position of a prior grain boundary is dotted according to the orientation measurements. The subgrain growth in the parent matrix took place only within the thickness of one subgrain. Besides, a band structure (parallel to RD) can be observed in the parent matrix (3~5) and normal subgrains in the consumed matrix (6~ 8). Such band structure in the parent matrix and confused subgrains in the consumed matrix were also found in other TEM examples and should be ascribed as a microstructural feature in two types of matrices.

3.3 Orientational characteristics of SIBM grains and their surroundings

From Figs. 3~ 6 it can be seen that SIBM grains are often *B/R* oriented. In order to obtain statistically more relevant information, from 61 SIBM grains selected from 26 cases in 80% rolled, 380 ℃ 20 s annealed sample A0 an ODF was computed (Fig. 7). It is evident that the SIBM grains are not randomly oriented as in the samples deformed at low or medium strains, but

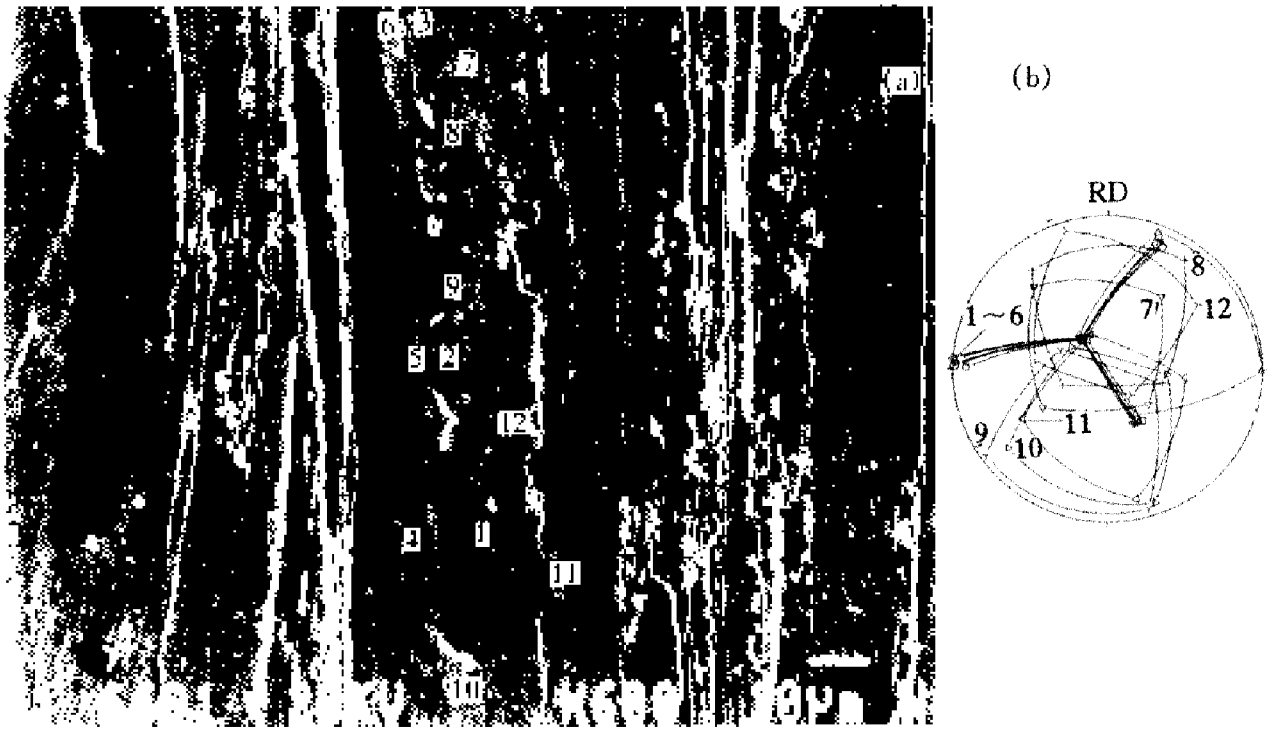

Fig. 4 A group of SIBM grains of 80% rolled and 380 ℃, 20 s annealed sample A0
(a) —Micrograph; (b) —(111) pole Fig.

Fig. 5 An example showing that SIBM grains can not grow into their complementary band of 80% rolled and 400 ℃, 10 s annealed sample A0
(a) —Micrograph; (b) —(111) pole Fig.

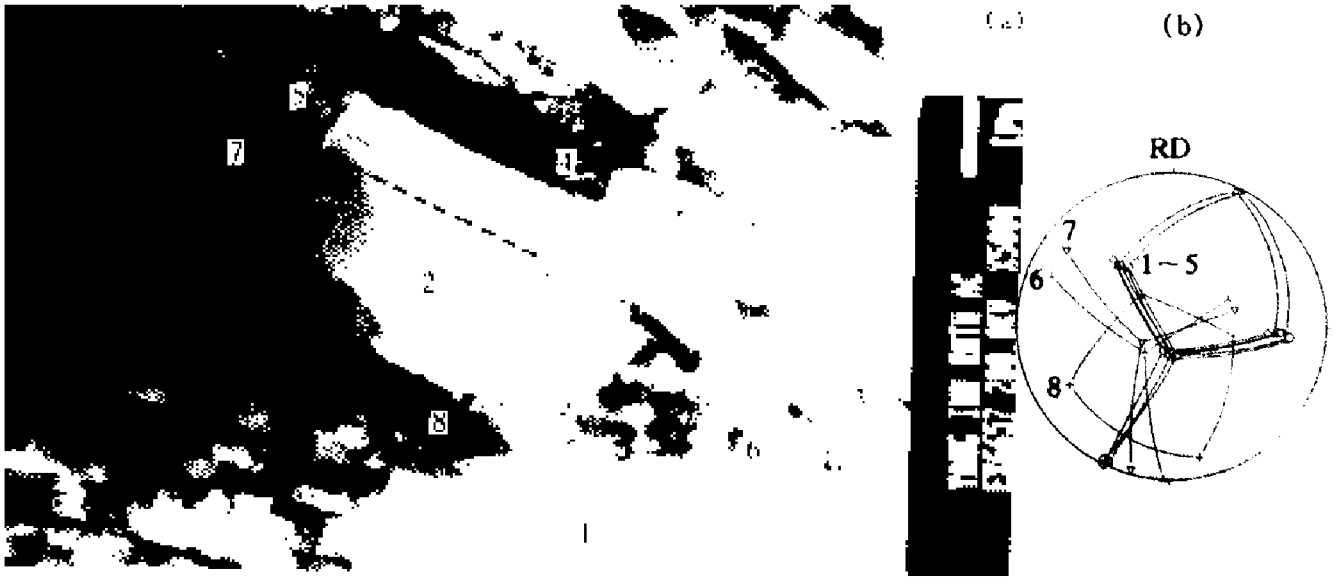

Fig. 6 TEM micrograph showing subgrains around an SIBM grain in 86% rolled and 388 ℃, 12 s annealed sample A0
(a) —Micrograph; (b) —(111) pole Fig.

they are all assembled along the rolling texture β-fiber with a significant preference for the *B* orientation.

The orientations of the parents of SIBM grains are similar to those of the SIBM grains. The orientations of the matrices consumed by SIBM grains are represented in Fig. 8. This ODF comprises the other orientations of the rolling texture except *B* and *G*, indicating that the *B*/*R* matrix can not be consumed by other orientations during SIBM and the *G* oriented subgrains do not participate in the SIBM process. Since the measured orientations came from the subgrains close to the grain boundaries in the consumed matrices, they do not show typical rolling texture orientations. Fig. 9 shows the distributions of rotation angles and rotation axes between SIBM grains and the matrices on both

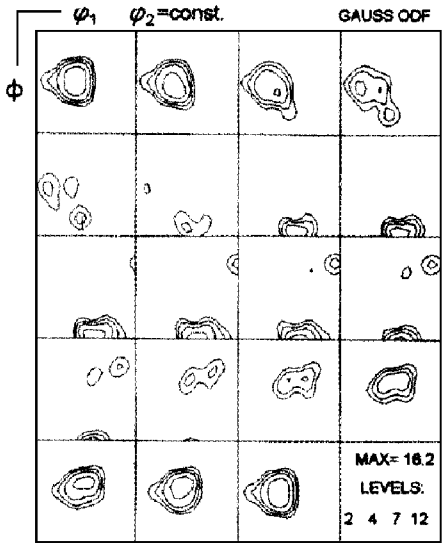

Fig. 7 Orientations of SIBM grains

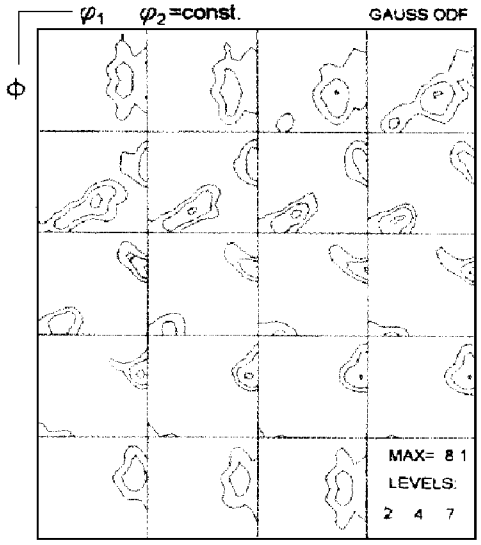

Fig. 8 Orientations of matrices consumed by SIBM grains of 80% rolled and 380 ℃, 20 s annealed sample A0

sides. The misorientations of SIBM grains with their immediate parents are mostly between 2°~ 6° with an average value of 4.9° (Fig. 9(a)), and the rotation axes are randomly distributed (Fig. 9(b)). The rotation angles of SIBM grains with the consumed matrix are quite large and between 24°~ 60° with an average value of 39.5° (Fig. 9(c)). The rotation axes reveal, although being nearly at random, a slight tendency of rotating towards the ⟨111⟩ axis (Fig. 9(d)). The misorientations within the parents and the consumed matrices of the SIBM grains (Fig. 10(a), (b)) (Without spatial relation, only distance and direction of measuring points were considered) reveal a large distinction which is related to the stored energy (Similar results were also found in different matrices during studying continuous recrystallization[15]). So, the stored energy in the *B* matrix is clearly lower than that in other oriented matrices.

4 DISCUSSION

The SIBM process in highly strained Al (alloys) with Fe, Mn in solution is differen from that in lowly strained pure Al as most commonly observed. The SIBM process prevails in lowly strained materials because grain boundaries are the sole type of nucleation sites and no other deformation inhomogeneities have been formed. In addition, no strong deformation texture can be formed at low strain and, consequently, no preferred orientations are expected to exist in the new grains formed at grain boundaries during annealing. In contrast to that, the SIBM process in combination with rolling orientations in newly recrystallized grains is always correlated with alloying/foreign atoms in solution, e g Fe, Si in 1*xxx* commercial pure Al[1-4] and Mn in 3*xxx* AlMn alloy[5-7]. It should further be stressed

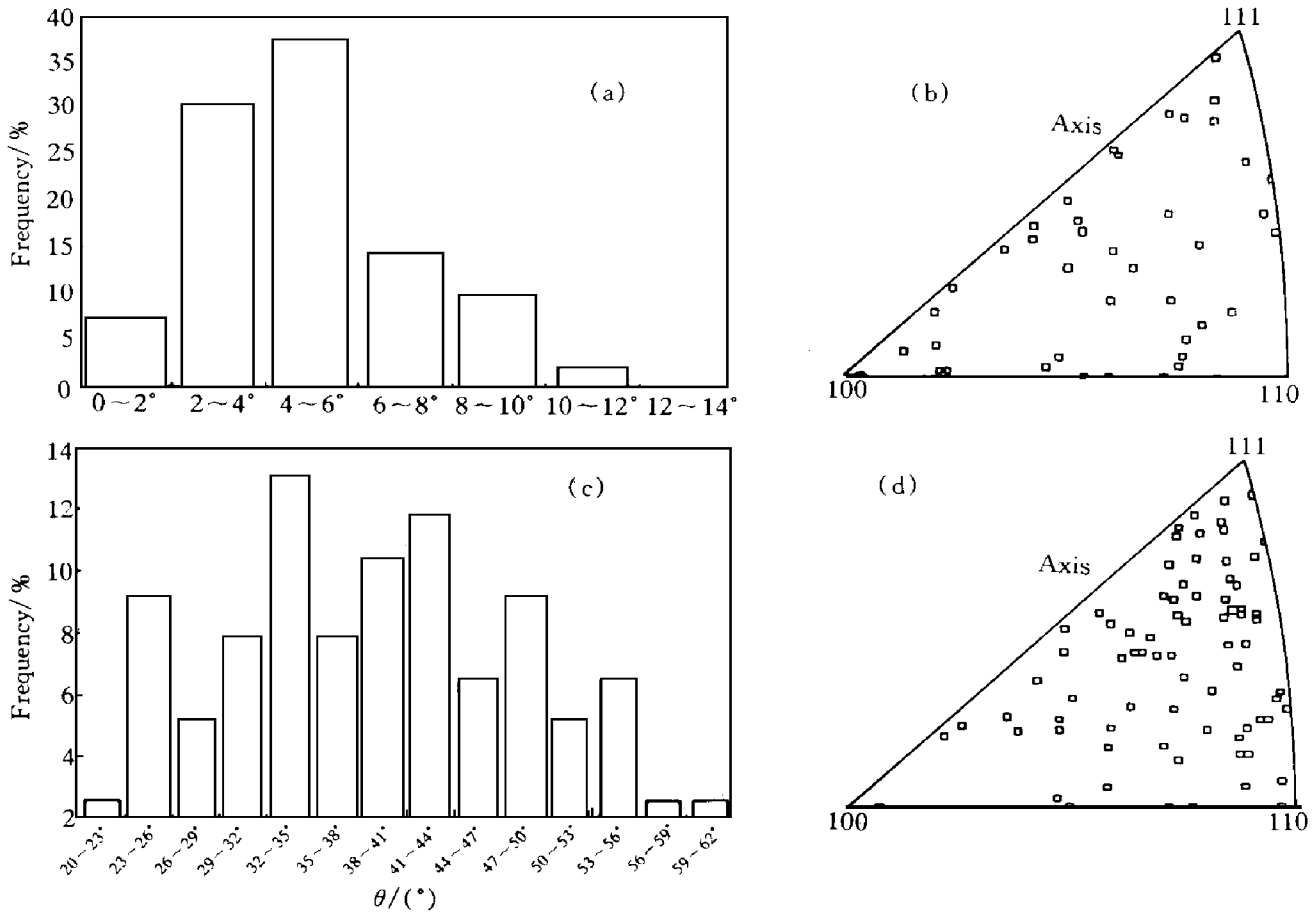

Fig. 9 Rotation axes and angles of SIBM grains with respect to both sides of their matrices
(a), (b) —Rotation angles and axes between SIBM-grains and consumed matrix, respectively
(c), (d) —Rotation angles and axes between SIBM-grains and consumed matrix, respectively

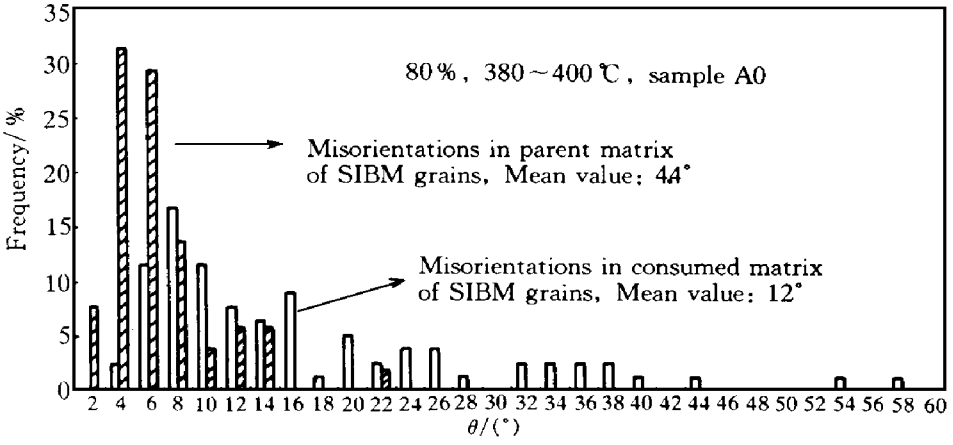

Fig. 10 Misorientations of subgrains in parent and consumed matrices of SIBM grains

that not all grains formed at grain boundaries have rolling orientations. An early classic work[16] revealed that two types of grains formed at boundaries. One is related to the SIBM grains growing only in one direction and the other deals with the randomly oriented grains which grow in both directions. The grains formed at grain boundaries with random orientation were also observed in Ref. [17]. Our results show that initial grain size affects the ratio of these two types of grains (Fig. 2).

According to Figs. 1, 2 large initial grain size, low annealing temperature and precipitation facilitated the formation of *B*/*R* component, whereas high strain favored both cube texture and *B*/*R* texture (Fig. 1). The influence of low annealing temperature is actually the same as precipitation. The stronger the precipitation is, the more the SIBM grains form. Large initial grain size has the effects of three folds. Firstly, at same strain the (sub) grains in fine grained samples experience larger rotations and store more strain energy than those in coarse grained samples. Thus, SIBM, which usually occurs in low strained materials, is more frequently observed in the latter. Secondly, the deformation behavior in coarse grained samples is expected to be different to that in fine grained samples. The deformation banding process takes place more frequently in coarse grained materials than in fine grained materials[18]. This indicates that at the same strain rate the grain rotations, particularly in the region close to the grain boundaries, are large in the samples with a small initial grain size, leading to more random orientations at the boundaries. In contrast to this, through frequent deformation banding, rolling orientations could be stable in the region near the boundaries in the samples A0 with a large initial grain size. Thirdly, a small initial grain size will give rise to more and thinner cube bands as nucleation sites and sharp orientation gradients across the cube bands, thus results in strong nucleation at the cube bands and disfavores SIBM process.

Although the nucleation of the grains with rolling orientations at low annealing temperatures is high (Fig. 2(a)), their growth is inferior to that of cube grains due to geological advantage of cube grains over *B*/*R* grains: cube grains originate from thin cube bands in deformed matrix[12, 19] and can grow in both directions normal to cube bands, while *B*/*R* grains can only grow in one direction. Moreover, because *B*/*S* components are main rolling texture components, there must be a lot of *B*/*S* deformation bands including both similar and complementary orientations *B*/*S*. They hinder the growth of new SIBM grains due to similar orientation or immobile, nearly twin relationship. So a high intensity of such texture component must be due to their strong nucleation ability and not their growth ability.

The smaller misorientation in *B*-oriented deformation bands in comparison to those of other orientations like *C* and *S* has already been found[20] and explained why most grains are *B*/*R*-oriented other than *C*-oriented. The key point is that the smaller misorientation is related

to less activated slip systems in B-matrix, and, therefore, less interaction between different slip systems and lower stored energy, providing a favorite condition for SIBM process.

As for the question why it is the R orientation and not the C or the B orientation that forms at grain boundaries in commercial $1xxx$ pure Al, this was ascribed[4] to the deformation behavior according to Taylor type models, namely, among the three complementarily oriented deformation bands, B/B', C/C' and S/S', the first two pairs have nearly 60° ⟨111⟩ stable, non-moving twin boundaries. Thus, preferred nucleation could only occur between the 40° ⟨111⟩ oriented S/S' bands. However, this is not observed in AlMn alloy and our explanation is that the low difference in stored energy between S and its complimentary S' deformation bands prevents nucleation. A recent study on S oriented bi-crystals[21] has shown that this type of grain boundary between S and S' is also stable and not suitable for nucleation.

Till now it is not fully understood how Fe, Mn atoms affect the growth of different types of grains. It was summarized[22] that the solute in solution might affect the behavior of the cube texture and rolling texture components in the following ways:

(1) Retarding the growth of cube grains;

(2) Enhancing the storage of dislocations during deformation and so providing better favorable conditions for the formation of nuclei of random or rolling texture orientations;

(3) Reducing the density of cube bands.

The first point is shared by many investigators. It was assumed[2] that Fe in solution affects the growth of cube grains stronger than that of R grains in Al.

In consideration of this, efforts are made to distinguish these assumptions, namely, by comparing the structural and orientational changes of 80% rolled samples A0 treated in the following ways:

(1) Annealing a sample at 350 ℃ for several days. Only several grains recrystallized discontinuously and grew preferentially in rolling direction. No precipitates were observed within the recrystallized grains, indicating that at this temperature, the growth of the new grains would stop if precipitation took place. The orientations of such grains reveal the preferred nucleation of grains with rolling texture orientations. This difference occurred before or at the early stage of precipitation.

(2) Annealing another sample at 450 ℃ for 10 s. About 10% of the sample's volume recrystallized. This sample was then annealed at 350 ℃ to observe the further growth of the new grains with different orientations. It is found that even after 3 d of annealing, the recrystallized grains are not able to grow further, i e precipitation stops the growth of grains with different orientations in the same way. In order to promote the growth of these recrystallized grains, the same sample was annealed at 450 ℃ for 3 min until recrystallization is completed. The grain size was heterogeneous showing a bimodal grain size distribution. Many small equiaxed grains, which formed during the first annealing at 450 ℃, could not grow and many large elongated grains nucleated directly from the deformed matrix even if tiny precipitates were distributed homogeneously in the matrix. The orientations of large grains were measured illustrating that no grains with a specific orientation can overcome the resistance of precipitation. No large difference, but a slight increase, in the number of cube grains is observed. However, it is noted that this was related to the influence of precipitation on nucleation and not on growth.

In summary, the influence of precipitation on different texture components should be traced to recovery processes and nucleation and not to the growth at a late stage. During the growth of new grains, the retardation of precipitation is independent of their orientations. It is assumed that the nucleation work for the SIBM process is lower than that of the cube grains. The B/R oriented subgrains need only to grow directly by boundary migration, while the cube subgrains must undergo recovery to gain a size advantage, that is, they have a longer incubation period. This recovery process is strongly retarded by Mn atoms through segregation at subgrain boundaries or dislocations. The grains formed at grain boundaries with random orientations are, like

the cube grains, similarly affected by this, leaving the SIBM process to be the very prominent one.

5 CONCLUSIONS

(1) The B/R texture component in recrystallized Al-1.3% Mn is caused by the grains formed at grain boundaries through the SIBM mechanism. Large initial grain size, more Mn atoms in solution and low annealing temperature favores its formation.

(2) The growth of such SIBM grains is inferior to that of cube grains because of their unidirectional growth and the restriction of large amount of similarly or complementarily oriented, deformed matrices. The formation of the B/R orientation at grain boundaries is not due to the preferential $40°\langle 111\rangle$ relationship between R and complementary R' orientation.

(3) A band-like microstructure is observed in the parent matrix of SIBM grains and a confused arrangement of subgrains is observed in the consumed matrix. Such microstructural difference is the reflection of smaller misorientations in the parent matrix and larger misorientation in the consumed matrix, indicating a low stored energy in the parent matrix and a stable B/R orientation even at grain boundaries (not rotated into random orientation). Thus, rolling texture orientations remains in the new grains formed at grain boundaries after recrystallization. The influence of Mn in solution on the formation of rolling orientations is attributed to its influence on recovery or nucleation, and not on the growth of differently oriented grains at the late stage of recrystallization.

REFERENCES

1 Grewen J and Heimendahl M V. Z Metallkde, 1968, 59: 236.
2 Ito K, Lücke K and Rixen R. Z Metallkde, 1976, 67: H.5, 338.
3 Ito K, Musick R and Lücke K. Acta Metall, 1983, 31: 2137.
4 Hirsch J and Lücke K. Acta Metall, 1985, 33: 1927.
5 Danh N C, Murakami T and Takahashi T. Trans Japan Inst Metals, 1980, 21: 401.
6 Bleck W and Bunge H J. Acta Metall, 1981, 29: 1401.
7 Ørsund R and Nes E. Scripta Metall, 1988, 22: 665.
8 Asbeck H O and Mecking H. Mater Sci and Eng, 1978, 34: 111.
9 Hirsch J, Burmeister G, Hoenen L *et al*. In: Bunge H J ed. Experiment Techniques of Texture analysis, DGM-Informations, Gesellschaff, Oberursel, 1986, 63.
10 Bunge H J. Quantitative Texture Analysis. Oberursel: DGM-Informations, Gesellschaft, 1981.
11 Engler O and Gottstein G. Steel Research, 1992, 63: 413.
12 Engler O, Yang P and Kong X. Acta Mater. 1996, 44: 3349.
13 Hirsch J and Lücke K. Acta Metall, 1988, 36, 2883.
14 Kong X W. Diploma Thesis, RWTH Aachen, 1986.
15 Engler O and Yang P. In: Hansen N *et al* eds. 16th Ris Ø Inter Symp Roskilde, Denmark, 335.
16 Beck P A and Sperry P R. J Applied Physics, 1950, 21: 150.
17 Vatne H E, Benum S, Shahani R *et al*. In: Hansen N *et al* eds. 16th Ris Ø Inter Symp, Roskilde, Denmark, 1996: 573.
18 Duggan B J, Sindel M, Köhloff G D *et al*. Acta Metall Mater, 1990, 38: 103.
19 Doherty R D, Samajdar I, Necker C T *et al*. In: Hansen N *et al* eds. 16th Ris Ø Int Symp Roskilde, Denmark, 1995: 1.
20 Driver J H, Juul Jensen D and Hansen N. Acta Metall Mater, 1994, 42: 3105.
21 Blicharski M, Liu J and Hu H. Acta Metall Mater, 1995, 43: 3125.
22 Hutchinson W B and Nes E. In: Hansen N *et al* eds. 7th Ris Ø Inter Symp Roskilde, Denmark, 1986: 107.

(Edited by Huang Jinsong)